Artificial turf infill associated with systematic toxicity in an amniote vertebrate

Elvis Genbo Xu[a], Nicholas Lin[a], Rachel S. Cheong[a], Charlotte Ridsdale[b], Rui Tahara[b], Trina Y. Du[b], Dharani Das[c], Jiping Zhu[c], Laura Peña Silva[a,b], Agil Azimzada[a,d], Hans C. E. Larsson[b,1], and Nathalie Tufenkji[a,1]

[a]Department of Chemical Engineering, McGill University, Montréal, QC H3A 0C5, Canada; [b]Redpath Museum, McGill University, Montréal, QC H3A 0C4, Canada; [c]Environmental Health Science and Research Bureau, Health Canada, Ottawa, ON K1A 0K9, Canada; and [d]Department of Chemistry, University of Montreal, Montreal, Quebec H3C 3J7, Canada

Edited by Catherine J. Murphy, University of Illinois at Urbana–Champaign, Urbana, IL, and approved September 30, 2019 (received for review June 8, 2019)

Artificial athletic turf containing crumb rubber (CR) from shredded tires is a growing environmental and public health concern. However, the associated health risk is unknown due to the lack of toxicity data for higher vertebrates. We evaluated the toxic effects of CR in a developing amniote vertebrate embryo. CR water leachate was administered to fertilized chicken eggs via different exposure routes, i.e., coating by dropping CR leachate on the eggshell; dipping the eggs into CR leachate; microinjecting CR leachate into the air cell or yolk. After 3 or 7 d of incubation, embryonic morphology, organ development, physiology, and molecular pathways were measured. The results showed that CR leachate injected into the yolk caused mild to severe developmental malformations, reduced growth, and specifically impaired the development of the brain and cardiovascular system, which were associated with gene dysregulation in aryl hydrocarbon receptor, stress-response, and thyroid hormone pathways. The observed systematic effects were probably due to a complex mixture of toxic chemicals leaching from CR, such as metals (e.g., Zn, Cr, Pb) and amines (e.g., benzothiazole). This study points to a need to closely examine the potential regulation of the use of CR on playgrounds and artificial fields.

artificial turf | amniote model | tire crumb | embryonic development | environmental health

Municipalities and schools are sometimes replacing natural grass fields and playgrounds with artificial turf, as the latter is cheaper, water saving, and easier to maintain. To date, there are over 11,000 synthetic turf athletic fields in the United States and over 13,000 in Europe (1). Crumb rubber (CR) particles obtained by shredding vehicle tires are commonly used as infill material for artificial turf. Concerns have been raised regarding the potential health hazards and environmental risks of a broad spectrum of toxic substances known to be released from CR (2). Risks associated with CR differ depending on the exposure route as well as a variety of environmental factors, including precipitation, heating/cooling cycles, ozone, oxygen, and UV light exposure that can accelerate the leaching of toxic chemicals from CR (3). A thorough and comprehensive risk assessment is urgently needed (4) and some federal agencies have recently begun research programs to address this issue (https://www.epa.gov/chemical-research/federal-research-recycled-tire-crumb-used-playing-fields).

Over 300 chemicals have been identified in CR, of which nearly 200 are predicted to be carcinogenic and genotoxic (1). The majority of these potential carcinogens are not listed in the databases of the United States Environmental Protection Agency (US EPA) nor the European Chemicals Agency (ECHA) due to the absence of toxicological evaluation (1). Our preliminary toxicity experiments with *Daphnia magna* indicate that CR water leachate causes immobility and mortality depending on leachate concentration (*SI Appendix*, Fig. S1). These findings align with the acute toxicity of CR reported in aquatic model organisms, such as alga, daphnia, amphibians, and fish as well as soil invertebrates (5–7). However, the impacts of CR exposure to higher vertebrates, including humans, are unknown. To address this critical knowledge gap, we developed an amniote vertebrate model to study toxic effects and mechanisms of CR toxicity.

The chicken embryo is an excellent higher vertebrate toxicological model for several reasons. The genomes of bird and mammal show little interspecific variation, and amniotes undergo no genome duplications (8, 9); the relative organ size (e.g., brain) development of chicken embryos is comparable to that of early mammals, including humans; early stage amniote embryos lack a blood–brain barrier; chicken embryos are sensitive to a range of environmental toxicants, which can be easily applied to the egg surface or injected into the air cell, yolk, or vasculature; and chicken embryos present ethical advantages avoiding sacrifice of pregnant animals prior to examination (10–12). We also benefit from an existing body of work on chemicals associated with general rubber products that were shown to be toxic in chicken models. However, past toxicological studies were largely limited to individual chemicals by *in ovo* injections with limited toxicity endpoints such as mortality and gross morphological deformities (10, 13). No detailed sublethal effects of the CR chemical mixture have been explored.

We exposed chicken embryos to CR-contaminated water (leachate) to reveal its systematic toxicity with particular emphasis on the brain and cardiovascular system. An adverse outcome pathway framework, including several molecular initiating events and phenotypic outcomes occurring at different levels of biological organization, was proposed as a causal model for the toxicity mechanism and to help guide future risk assessments on CR. Moreover, in this case study with CR, we demonstrated the utility of chicken embryos as an appropriate amniote vertebrate model for systematic toxicity evaluations of other environmental contaminants.

Significance

Athletes and children are playing on artificial turfs. However, the health risk associated with exposure to crumb rubber from artificial turfs is unknown for higher vertebrates. Here, we employed chicken embryo as a developing amniote vertebrate model to show that toxic leachate from artificial athletic turf infill impairs the early development of chicken, notably brain and cardiovascular system. This study triggers a scientific discussion as to whether crumb rubber is an appropriate infill material for artificial fields.

Author contributions: E.G.X., N.L., J.Z., L.P.S., H.C.E.L., and N.T. designed research; E.G.X., N.L., R.S.C., C.R., R.T., T.Y.D., D.D., L.P.S., and A.A. performed research; E.G.X., N.L., R.S.C., C.R., R.T., T.Y.D., D.D., J.Z., A.A., and H.C.E.L. analyzed data; and E.G.X., N.L., J.Z., H.C.E.L., and N.T. wrote the paper.

Competing interest statement: The authors declare no competing interest.

This article is a PNAS Direct Submission.

Published under the PNAS license.

[1]To whom correspondence may be addressed. Email: hans.ce.larsson@mcgill.ca or nathalie.tufenkji@mcgill.ca.

This article contains supporting information online at https://www.pnas.org/lookup/suppl/doi:10.1073/pnas.1909886116/-/DCSupplemental.

First published November 25, 2019.

Results

Growth and General Morphology. Prior to incubation, chicken embryos were exposed to CR water leachate in 4 ways: coating of the eggshell surface with CR leachate (coating), dipping the intact egg into CR leachate (dipping), direct injection of the CR leachate into the yolk (inject-Y), or direct injection into the air cell (inject-A). CR leachate did not cause significant mortality of embryos in the first 7 d of incubation (embryonic day, E7) for all treatments (*SI Appendix*, Fig. S2*A*). However, embryos treated with CR leachate by dipping and injection lost more mass than controls (Fig. 1*A*). No severe abnormal features were observed with coating exposure. Only 1 embryo of 30 was malformed after dipping exposure, and only 1 of 15 after injection into the air cell (inject-A). In contrast, over half (8/15) of the yolk-injected (inject-Y) embryos developed severe malformations (Fig. 1*B* and *SI Appendix*, Fig. S2*B*). By E7, most chicken embryos normally developed to an anatomical stage 29–30 (*SI Appendix*, Fig. S2*C*) (14). The developmental stage was not significantly affected by CR treatment, except for 2 embryos from the inject-Y group that only developed to stages 21 (with faint eye pigmentation) and 27 (with barely recognizable beak) (*SI Appendix*, Fig. S2*C*). Embryos that survived to E7 without severe abnormal malformations were further measured for the eye area, midbrain area, head size, and body length. No significant difference was detected between control and coating groups (Fig. 1*C*). Dipping exposure resulted in embryos with significantly smaller eyes and midbrain areas than controls (Fig. 1*C*). Inject-Y embryos also had a significantly smaller midbrain area than controls (Fig. 1*C*). This treatment did not induce asymmetry of limb length development but significantly reduced the limb lengths (*SI Appendix*, Fig. S2*D*). Given that inject-Y was the treatment that consistently induced the most pronounced changes in all morphology measurements, further analyses below were focused on the inject-Y embryos to reveal the detailed sublethal effects and potential toxicity mechanisms.

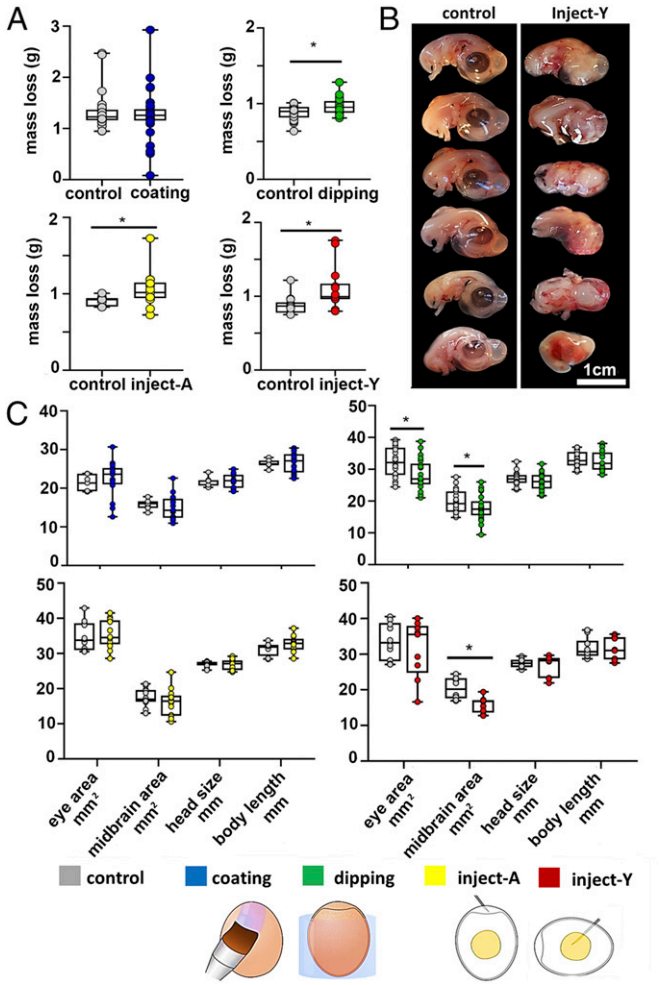

Fig. 1. The effects of CR water leachate on the growth and general morphology of E7 chicken embryos. (*A*) Egg mass loss. (*B*) Embryos exhibit severe malformations after inject-Y treatment. (*C*) Measurements of the eye area, midbrain area, head size, and body length of CR-treated and control embryos. Inject-A, E0 embryos were injected with CR leachate into the air cell; inject-Y, E0 embryos were injected with CR leachate into yolk; control E0 embryos were treated with LC/MS grade water with the treatment-equivalent methods. *$P < 0.05$ (*t* test; $n = 30$ for coating and dipping, $n = 15$ for inject-A and inject-Y).

Brain Morphology. Brain development was adversely affected by CR leachate (Fig. 2 *A* and *B*). Although total brain volume was not significantly affected by inject-Y treatment (Fig. 2*C*), significant reductions in the frontal lobe height (Fig. 2*D*) and midbrain-mesencephalon cleft (Fig. 2*E*) were detected. Other 2-dimensional (2D) linear parameters were not different from controls (Fig. 2*B*). The 3-dimensional (3D) comparisons between controls and inject-Y brains revealed multiple regions of differential effect. Notably, the external surfaces of the entire telencephalon, ventral region of the infundibulum, and lateral regions of the mesencephalon were reduced in size by over 100 microns in the inject-Y embryos compared to controls (Fig. 2*F*). Additionally, the internal surfaces of the lateral mesencephalon were also reduced, and the tissue thickness of the brain was reduced in the dorsal telencephalon, lateral diencephalon, and posterodorsal mesencephalon (Fig. 2*F*).

Blood Vessel Development and Heart Rate. Extraembryonic angiogenesis and heartbeat rate in E3 embryos were affected by CR treatment. The control group developed normal, highly branched vasculature (Fig. 3*A*), whereas the inject-Y embryos had significantly reduced vascular density and distal branching (Fig. 3*B*), indicating an antiangiogenic potential of CR leachate. The inject-Y embryos also had significantly lower heartbeat rates with higher variation than the controls (Fig. 3*C*).

Gene Expression. The expressions of biomarker genes specific to different biological pathways were assessed in the brain, liver, and heart of E7 embryos (Fig. 3*D*). The expression of four selected genes that play central roles in the thyroid hormone pathway, including transthyretin (TTR), thyroid hormone receptors (TRα, TRβ), and neurogranin (RC3), were compared between different treatments of CR leachate with controls. Only the injection treatment significantly suppressed the RC3 gene, while the TTR gene was consistently up-regulated by all CR treatments (Fig. 3*D*), suggesting the presence of TTR-binding compounds in the leachate. Expression of hepatic aryl hydrocarbon receptor (AHR) and metallothionein (MT1) transcripts was up-regulated by injection treatments compared with controls, while P450 genes (CYP1A4, CYP1A5) were down-regulated (Fig. 3*D*). These genes are known to be involved in the regulation of biological responses to aromatic (aryl) hydrocarbons and metals, as well as in apoptosis. Similar to the gene expression results in the liver, MT1 transcripts in the heart were significantly up-regulated by all CR treatments (mean fold change > 8). Other stress-response genes (HSP60, HSP70, CYP1B1) were also up-regulated with the largest response to inject-Y (Fig. 3*D*).

Toxic Compounds. A comprehensive evaluation of the soluble chemicals leached from the CR was beyond the scope of this study; however, targeted analyses were performed to quantify the levels of toxic metals and amines. Several metal ions leached from CR, with Zn being the most abundant (>5 mg/L), followed by Cu. The average extent of leaching, in the order of abundance, was Zn

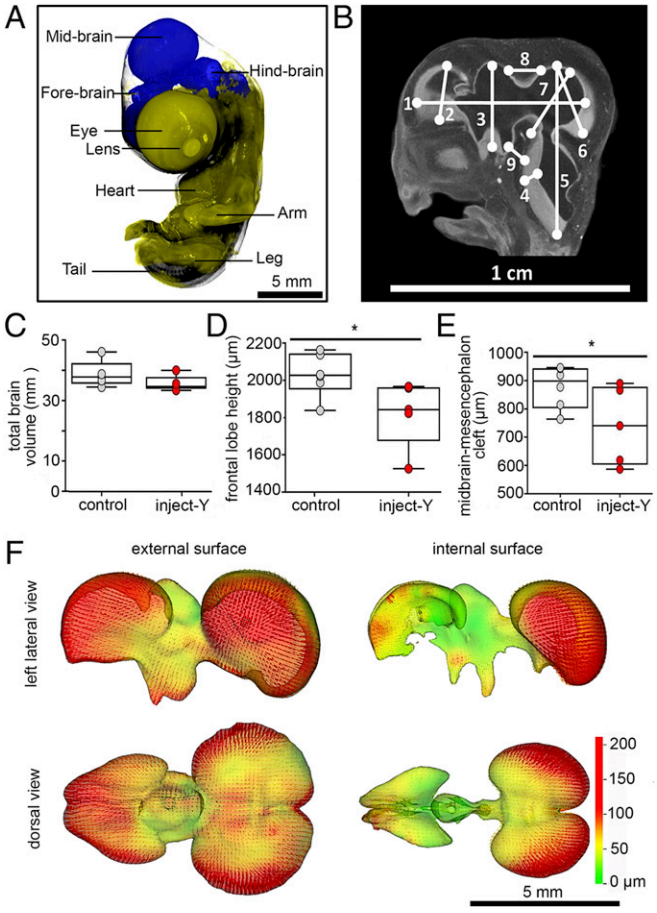

Fig. 2. Brain morphology of E7 chicken embryos. (*A*) A 3D view of an E7 embryo with a highlighted brain. (*B*) Nine 2D linear measurements on brain section (1, total brain anterior-posterior length; 2, frontal lobe height; 3, midbrain height; 4, rhombencephalon thickness; 5, rhombencephalon height; 6, mesencephalon height; 7, mesencephalon thickness; 8, midbrain-mesencephalon cleft; 9, midbrain-rhombencephalon cleft). (*C*) Total brain volume. (*D*) Frontal lobe height. (*E*) Midbrain-mesencephalon cleft (*$P < 0.05$; *t* test; $n = 5$). (*F*) Differences of 3D brain external and internal surface morphology between control and inject-Y ($n = 6$). Control, E0 embryos were injected with LC/MS grade water into yolk. Inject-Y, E0 embryos were injected with CR leachate into yolk. All deformations are inward.

(5,156.26 μg/L) >> Cu (7.47 μg/L) > Al (5.71 μg/L) > As (2.32 μg/L) > Cr (1.81 μg/L) > Pb (0.29 μg/L) >> Cd (0.02 μg/L) (*SI Appendix*, Table S1). Zn, Cu, Cr, and Pb were also detected in the albumin, yolk, liver, heart, and brain of inject-Y embryos at higher concentrations than controls in most cases (*SI Appendix*, Fig. S3). The concentration of Zn in the liver of inject-Y embryos (37.54 μg/g) was significantly higher than that of control embryos (9.53 μg/g) (*SI Appendix*, Fig. S3*A*). The highest concentrations of metals were consistently found in liver and yolk with Zn being the most abundant (*SI Appendix*, Fig. S3*A*). A number of amines (from C_6 to C_{13}) were detected in CR leachate with *N*-cyclohexyl-cyclohexanamine (40.5%; 4,113 μg/L), hexa(methoxymethyl)melamine (17.1%; 1,735 μg/L), and benzothiazole (14.9%; 1,511 μg/L) found at the highest concentrations (*SI Appendix*, Table S2).

Dose–Response Effects. Adverse responses such as abnormal development and decrease in heartbeat rate became greater with increasing CR leachate concentrations (*SI Appendix*, Figs. S4 and S5). Similar to 100% leachate, both 25% and 50% leachate led to up-regulation of TTR and HSP60 gene but down-regulation of CYP1A4 gene (*SI Appendix*, Fig. S5). Benzothiazole exposures reproduced multiple toxic effects that were similar to CR leachate exposure, including reduced heartbeat rate, down-regulation of CYP1A4 and CYP1B1, and similar malformations such as delayed development and embryos without eyes (*SI Appendix*, Figs. S4 and S5). This suggests that benzothiazole is a toxic chemical associated with the observed CR leachate toxicity.

Discussion

Precipitation on outdoor artificial athletic fields could lead to leaching of CR infill that may be an important exposure route to environmental species and humans as a result of freshwater contamination. Our study revealed that the CR leachate had a system-wide effect on developing chicken embryos. This demonstrates the CR toxicity on higher vertebrates. The adverse developmental effects were more pronounced for the yolk injection treatment compared to the 2 surface exposure methods and air cell injection. Of note is that over half of the inject-Y embryos were not expected to be viable at a later developmental stage due to the severe whole-body malformations. Additionally, failure of the extraembryonic vasculature to develop distal branches may indicate a disruption in the HIF-1/VEGF/TIE pathway (15). With the current data, the question of whether and how this pathway is disrupted by CR leachate exposure remains unsolved. However, some insights can be obtained from the dose–response data. *SI Appendix*, Fig. S5 *A* and *B* indicates that the blood vessel development was not significantly affected by benzothiazole at 1.5 mg/L and 15 mg/L. This suggests that either some other chemicals leached from CR may cause the failure of the extraembryonic vasculature to develop distal branches or the concentrations of benzothiazole are below a development threshold. Future studies integrating results from toxicity identification evaluation (16), real-time observation of embryonic angiogenesis, and nontargeted chemical analysis would be necessary to answer the questions on the mechanism of the disruption in extraembryonic vessel development by CR leachate. Higher concentrations of metals were detected in the yolk of the

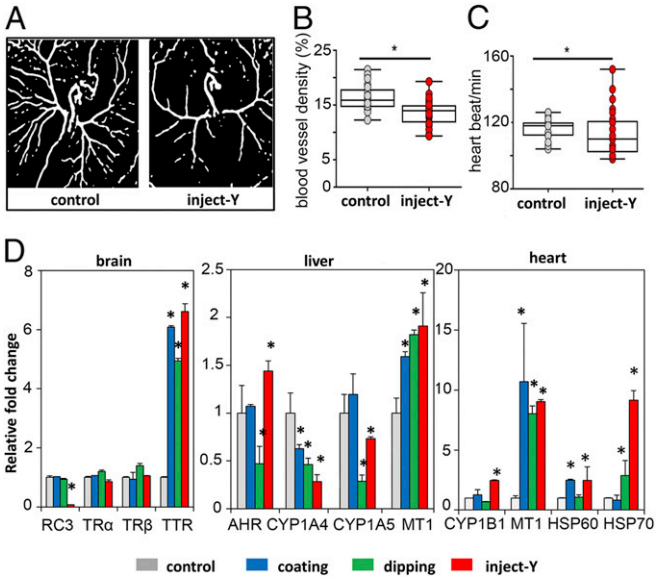

Fig. 3. The effects of CR water leachate on embryonic angiogenesis, heartbeat, and gene expression of chicken embryos. (*A*) Representative images of developing blood vessels of control and inject-Y E3 embryos. (*B*) Blood vessel density of E3 embryos. (*C*) Heartbeat rate of E3 embryos. Control, E0 embryos were injected with LC/MS grade water into yolk; inject-Y, E0 embryos were injected with CR leachate into yolk. *$P < 0.05$ (*t* test; $n = 30$). (*D*) Gene expression in brain, liver, and heart of E7 embryos. *$P < 0.05$ (1-way ANOVA followed by Bonferroni's *t* test; $n = 6$).

treated embryos than that of controls. Deposition of lipophilic organic compounds is also expected to be concentrated in the yolk (17) followed by transport to other tissues and organs during embryonic development. Brain formation was specifically affected by reduced development of the telencephalon, infundibulum, and mesencephalon. Specific regions within these portions of the brain could not be assessed by this early stage of development. However, functional outcomes could be predicted based on the known functions of these portions. The telencephalon controls voluntary motor functions, sensory processing, and complex cognitive processes; the infundibulum regulates metabolic processes; and the mesencephalon is associated with visual and motor system pathways (18). The common functions of these regions across vertebrates suggest that motor control, metabolism, sensory processing, and potentially cognition could be impaired if the chickens were brought to hatching.

Several metal ions detected in CR leachate were elevated in tissue samples of CR-treated chicken embryos, with Zn being the most abundant (*SI Appendix*, Fig. S3). Previous work identified Zn as the highest leachable metal in extracts of rubber materials due to the common application of zinc oxide as a vulcanization activator during the manufacturing of tire rubber, at an approximate concentration of 1.5% (5, 19). Zn was also identified as a major toxicant from CR to both aquatic and soil organisms (6, 7). Zinc toxicity has been widely linked to hepatotoxicity and shown to induce histological changes in the brain, suggesting its neurotoxicity is probably mediated by free radical injury (20). Avian studies have shown mild to severe degenerative abnormalities of the pancreas and teratogenic and reproductive effects associated with toxic Zn concentrations in the liver and pancreas (21). Those Zn concentrations were in the same range as those measured in our study.

In the inject-Y embryos, we detected brain differences and dysregulation of thyroid hormone pathway-associated genes, which play important roles in brain neural migration and differentiation (22). Although thyroid hormone concentrations were not quantified in this study, it is possible that the impaired brain development of chicken embryos may be caused, in part, via Zn-mediated disruption of the thyroidal pathway and function (23). The tissue levels of Cu (0.44–2.69 μg/g), Cr (0.43–1.61 μg/g), and Pb (0.0014–0.019 μg/g) were much lower than that of Zn (1.86–73.47 μg/g), but their potential additive contribution to the observed toxicity cannot be ignored (24). Although the tissue level of other metals was similar to the controls, their average concentrations in CR-treated embryos trended higher in yolk and heart than those of controls (*SI Appendix*, Fig. S3). It is possible that a portion of metals leached from CR was sequestered in the yolk, while a portion of free metals was absorbed by the embryos and transported to other organs via blood circulation after 7 d of development. Importantly, we do not exclude the possible contribution of other metals to the overall toxicity, because the mixture of metals could lead to additive or even synergistic toxic effects and the toxic action can be interdependent. This has been shown in different organisms both in vivo and in vitro (25–28). Furthermore, the significant up-regulation of heat shock proteins, which function to protect organisms from heavy metal pollution and oxidative stress (29), as well as metallothioneins, which are important proteins that protect against toxic metals (30), suggests metal intoxication or detoxification processes were activated upon exposure to CR leachate.

The water dissolved organic portion of CR contains various vulcanization stabilizers and accelerators as well as degradation compounds from rubber/tire manufacturing such as amines, aniline, quinoline, amides and benzothiazole (31). Although the toxicity of many of these compounds on the vertebrate embryo is largely unknown, 5 amines associated with CR demonstrate relatively high toxicity in the invertebrate *D. magna*, including *N*,*N*′-diphenyl-guanidine (LC_{50} 17 mg/L), cyclohexylamine (LC_{50} 80 mg/L), *N*-butyl-L-butanamine (LC_{50} 160 mg/L), benzothiazole (LC_{50} 160 mg/L), and hexa(methoxymethyl)melamine (LC_{50} 160 mg/L) (Ecotox Database, US EPA). Among them, benzothiazole has the potential to be mutagenic and carcinogenic (32). Therefore, in this study, we searched for and confirmed the presence of these amines in CR leachate as they are likely partially responsible for the observed toxicity. It is worth noting that some amines could be metabolized with a relatively short biological half-life, which makes the quantification of the parent compounds in embryo tissues not practical or rational after the 7-d exposure. For example, *N*,*N*′-diphenyl-guanidine has a half-life of only ∼9.6 h (TOXNET database, NIH). Therefore, some unknown metabolites could also accumulate and contribute to the toxicity.

The expression of hepatic AHR transcripts was up-regulated by 1.5-fold after 100% leachate injection treatment compared with control (Fig. 3*D*), but lower leachate concentrations (25% and 50%) did not induce a significant up-regulation of AHR (*SI Appendix*, Fig. S5*E*). This may suggest that the present AHR agonist in the leachate is weak. It is well known that the activation of AHR can further induce the expression of its target genes such as P450 genes in response to a variety of endogenous and xenobiotic chemicals (33). In the present study, CYP1A4 and 1A5 were down-regulated by leachate treatment (*SI Appendix* and Fig. 3*D*). It is possible that chemicals in the leachate suppress the expression of CYP1A4 and 1A5 via AHR-independent pathways (34). For example, previous studies found that transcriptional effects of metals (As, Pb, Hg, and Cd) on the decrease in CYP1A1 are mediated via factors acting at upstream region of the promoter, independently of the AHR (35, 36). Jacobs et al. (37) also confirm that CYP1A4 and 1A5 are inhibited by sodium arsenite at the level of transcription. Although the chemicals in the leachate that are responsible for the CYP1A genes down-regulation remain to be determined, the effect may be also mediated via cytokines that have been shown to down-regulate CYP1A (38, 39). Additionally, a number of studies linked CYP to apoptosis pathways. CYP inhibition can protect against oxidative stress-induced apoptosis that is associated with the Ca^{2+} influx changes and calpain (40). Thus, the up-regulation of AHR and down-regulation of CYP1A observed may be an indicator of immune responses caused by complex chemicals in the leachate. Increasing studies suggest that AHR plays an important role in regulation of immune responses. Indeed, Prigent et al. (41) observed AHR up-regulation after T cell activation, confirming AHR as an immediate-early activation gene. In a chicken study, an immunotoxin T-2 caused significant down-regulation of CYP1A4, 1A5, and 3A37 in liver and a similar decrease of CYP1A was also reported in rabbits (42, 43). Results of these studies on the up-regulation of AHR and down-regulated CYP1A genes are in accordance with our results, suggesting that AHR pathway, as well as other signaling pathways that are not initiated by AHR binding, could be both involved in response to CR leachate exposure.

Existing risk assessments of artificial athletic turf or CR have suggested low or negligible environmental and human health risks (2–5). However, none of these studies used a vertebrate model. Human health assessments often focused on youth or adult professional players, but the potential risk to younger children could be higher due to their earlier stage of development and frequent hand and facial ground contact. Moreover, the risk to human embryos via maternal exposure to CR is unknown. Environmental risk assessments are usually based on acute toxicity tests with invertebrate species on limited simple toxicological endpoints such as mortality. Chronic tests of CR on vertebrate species are lacking but critically needed because the release of toxic chemicals from CR is continuous and the leaching of contaminants from aging CR can be significant over the field's functional lifetime. Zinc and polycyclic aromatic hydrocarbons are among the most frequently studied chemicals in CR risk assessments. However, the risks of a large number of other chemicals frequently associated with CR are not assessed due to limited toxicological data. Using the chicken

embryo model, we provide comprehensive information to fill many of the gaps mentioned above by integrating chemical and toxicological data at different levels of biological organization of early development, via quantitative measurements in gene regulation, brain morphology, blood vessel development, cardiac physiology, and individual growth and malformation (*SI Appendix*, Fig. S6). The utility of these mechanistic data can be valuable as an aid to the selection of toxicity endpoints/biomarkers (e.g., heartbeat rate, TTR gene expression), the selection of developmental stage for testing, and the potentially responsible chemicals (e.g., benzothiazole) for more refined CR risk assessment. The plausible connections from gene dysregulation to individual malformation induction provide a critical foundation for development of future predictive approaches and also identify specific linkage gaps (e.g., gap between TTR gene expression in brain and midbrain development) that could not be filled by the present data. Finally, the use of the chicken embryo model offers a general tool to predict the potential impacts of other environmental pollutants and further expand the experimental repertoires used for risk assessment and regulatory application.

Materials and Methods

Leachate Preparation and Animals. Forty grams of CR for artificial athletic turf infill use was added to 500 mL of water (Optima LC/MS grade, Fisher Scientific) in clean glass amber bottles. After 1 wk of extraction with gentle shaking at room temperature, the leachate was filtered through a 0.22-μm cellulose acetate filter (Corning) to ensure debris, suspended solids, or microbial contaminants were eliminated. The conductivity of the leachate was measured using Accumet Basic AB 30 Conductivity Meter (Fisher Scientific), and the pH of the leachate was measured using Accumet Basic AB 15 pH Meter (Fisher Scientific). The measured values are provided in *SI Appendix*, Table S3.

Fertilized chicken eggs were weighed and transferred randomly to laboratory incubators. The incubators were maintained at 37–38 °C with ∼60% humidity. A fan within the incubator ensured oxygenated and homogeneous conditions. Water containers within the incubators were refilled once every 2 d, and incubators were tilted daily. Eggs were candled every day to verify viability and identify the stage of development.

Seven-Day Exposures. E0 chicken embryos were exposed to 100% (80 g/L) CR leachate using different approaches (Fig. 1), i.e., (*i*) coating by dropping 1 mL of CR leachate on the eggshell using a pipetter; (*ii*) dipping the eggs (to just below the air cell) into CR leachate for 30 s; and, *(iii)* microinjecting 12 μL of CR leachate into the air cell (inject-A) or yolk (inject-Y) using sterile 1-mL syringes. The first 2 approaches were designed to mimic external exposure in the natural environment, while the latter 2 aimed to mechanistically understand the toxicity of CR leachate. Each treatment has 3 replicates (incubators) with 10 eggs per replicate. Control embryos were treated with liquid chromatography/mass spectrometry (LC/MS) grade water with the treatment-equivalent methods. After 7 d, the masses of eggs were recorded and the E7 embryos were carefully extracted. Seven-day incubation was chosen due to the prominent midbrain, clearly demarcated limbs, and proper size of liver developed at the E7 stage for easy imaging, dissection, and measurements. Images were taken using a flat-field macrolens Sony α5000 digital camera for gross morphological measurement in ImageJ software (NIH). Yolk, albumin, liver, heart, and brain tissues were collected and stored in 2-mL centrifuge tubes at −80 °C for future chemical and molecular analyses.

Three-Day Exposure. A separate 3-d exposure was conducted to investigate the impacts of CR leachate on the cardiovascular development of chicken embryos due to the ease of access to the heart and blood vessel system at this stage. The same volume of 100% CR leachate (12 μL) was injected into the yolk of E0 chicken embryos. Each treatment has 3 replicates with 10 eggs per replicate. Control eggs were treated the same way with LC/MS grade water. After 3 d, eggs were removed from the incubator and placed on a heat block set at 38 °C. Video recordings were made through a circular window of ∼3 cm diameter cut in the shell over the embryo using a Sony α5000 digital camera. The embryos were allowed 1 min to acclimate prior to being recorded. Heart rate was measured during the first 30 s of each video. Images were also captured from the videos to quantify blood vessel density using Vessel Analysis plugin in ImageJ.

Dose–Response Exposure. To better explain the toxicity of CR leachate, 2 separate dose–response experiments (i.e., 7-d and 3-d exposure) were conducted. E0 chicken embryos were exposed to LC/MS grade water (control), 25% CR water leachate, 50% CR water leachate, 1.5 mg/L benzothiazole (BTZlow), and 15 mg/L benzothiazole (BTZhigh). The tested concentrations of CR leachate were determined based on the dose–response acute toxicity screened using *D. magna* assay that showed immobility when exposed to 25% and above CR water leachate (*SI Appendix*, Fig. S1), and 1.5 mg/L of benzothiazole was chosen in accordance with the concentration detected in the 100% CR leachate (1,511 μg/L). The conductivity of the diluted leachate was measured using Accumet Basic AB 30 Conductivity Meter (Fisher Scientific), and the pH of the diluted leachate was measured using Accumet Basic AB 15 pH Meter (Fisher Scientific). The measured values are provided in *SI Appendix*, Table S3. Twelve microliters of exposure solution was injected into the yolk of E0 embryos with 12 animals per treatment. After the exposure, imaging, video recording, tissue extraction, and analyses were performed following the same methods described above.

Nano-CT Scan. Nano-CT scans using Zeiss Xradia 520 Versa (Carl Zeiss Canada Limited) were performed on randomly selected E7 embryos that were not grossly deformed to quantify the impact of CR on brain development. Nano-CT was used to retain samples with soft tissue dimensions most similar to their original state, rather than the typically shrunken dimensions that result from tissue processing for whole mount light microscopy or histology (44). The embryos were extracted, washed in 0.01 M PBS, fixed in Bouin's solution for 45 min, then stored in 70% ethanol until staining. Embryos were removed from ethanol and stained in 1 or 2% phosphotungstic acid solution (phosphotungstic acid dissolved in 70% ethanol) for 7 d. After staining, the samples were embedded in 10-mL tubes with 0.5 or 1% agarose. The scanned samples were analyzed with Dragonfly image analysis software (Object Research Systems Inc.). Details of the Dragonfly method are provided in *SI Appendix*.

Gene Expression. National Center for Biotechnology Information (NCBI) nucleotide database was mined for chicken sequences of selected genes in the AHR pathway (CYP1A4, CYP1A5, CYP1B1, AHR1), stress-responsive genes (HSP60, HSP70, MT1), and genes associated with the thyroid hormone pathway (TRα, TRβ, TTR, RC3). Real-time qPCR primers were designed with PrimerQuest Tool (https://www.idtdna.com/site/account/login?returnurl=%2FPrimerquest%2FHome%2FIndex) (*SI Appendix*, Table S4). Designed primers were target-verified by NCBI Primer-BLAST. RNA was extracted from embryo samples using PureLink RNA Mini Kit (Life Technologies), following the instruction of the manufacturer including on-column digestion of DNA. The purity and concentration of total RNA were measured using a spectrophotometer ($OD_{260/280} > 1.8$; concentration > 800 ng/μL). The integrity of total RNA was assessed by 1% agarose gel electrophoresis. cDNA was synthesized from 200 ng of total RNA using the M-MLV Reverse Transcriptase kit (Thermo Fisher Scientific) following the instruction of the manufacturer. Gene expression was quantified using Power SYBR Green QPCR Master Mix (Life Technologies) per manufacturer's instruction. RT-PCR was performed on the 7900HT Fast Real-Time PCR System (Applied Biosystems) with the following protocol: 1 cycle at (*i*) 95 °C for 10 min; 39 cycles at (*ii*) 95 °C for 1 min; (*iii*) 55 °C for 30 s. Following the amplification reaction, a melting curve analysis was carried out between 60 and 95 °C, and fluorescence data were collected at 0.5 °C intervals. Relative qPCR expression was determined using $2^{-\Delta\Delta Ct}$ and normalized to the transcript levels for EF1A. A 1-way ANOVA followed by Bonferroni's *t* test for multiple comparisons versus control was performed to determine statistically significant differences in mRNA abundance between treated embryos and controls. Changes were considered statistically significant when $P < 0.05$.

Determination of Metals. Inductively coupled plasma mass spectrometry (ICP-MS) (NexION 300X, PerkinElmer) was used to determine the metal content (Al, Cr, Cu, Zn, As, Cd, and Pb) in the CR leachate and embryonic tissue samples. Details of the ICP-MS method are provided in *SI Appendix*.

Extraction of Organic Chemicals from CR Leachate for Qualitative Gas Chromatography and Mass Spectrometry Analysis. Three milliliters of dichloromethane (DCM; Sigma-Aldrich) were added to 45 mL of CR leachate (pH 7) in a 50-mL clear glass vial that had been precleaned by acid wash. The mixture was manually shaken and then sonicated in a bath sonicator (Branson 5510) for 10 min. The mixture in the vials was allowed to stand for 30 min and then centrifuged to separate the 2 layers at 1500 × *g*. The DCM layer was transferred using a Pasteur pipette into a 4-mL vial containing ∼2 g of anhydrous Na_2SO_4 and was allowed to stand for 2 h. Afterward, 50 μL of the DCM solution was transferred into a 200-μL insert that was placed in a GC vial for gas chromatography and mass spectrometry (GC/MS) analysis. Two hundred milligrams of Na_2CO_3 (Sigma-Aldrich) was added to the remaining

aqueous layer to bring the pH of the solution to 10. Then, the chemicals from the aqueous samples were extracted by repeating the procedure described above. A blank sample was prepared by taking 45 mL of LC/MS grade water instead of the leachate sample and following the same procedure as described above.

Extraction of Amines from CR Leachate for Quantitative GC/MS Analysis. An internal standard aniline-d_5 (250 ng) was added to 10 mL of CR leachate in a clear screw cap vial (15 mL size; Chromatographic Specialties). The solution was manually shaken for 1 min, followed by the addition of 2.5 mL of diethyl ether. The mixture was then manually shaken 2 times (3 min each time). The mixture was allowed to stand for 30 min and then centrifuged at 1,500 × *g* for 5 min to separate the 2 layers. The top diethyl ether layer was transferred carefully using a Pasteur pipette. Fifty microliters of this extract was transferred into a 200-μL insert that was placed in a GC vial for quantitation using GC/MS. A 6-point calibration curve was developed by spiking required amounts of amine mixture standards to 10 mL of LC/MS grade water and carrying out the same extraction procedure as described above for the samples.

GC/MS Analysis. GC/MS analysis was carried out using an Agilent gas chromatograph (Model: 7890A) connected to a Triple-Quad mass spectrometer (Agilent Technology Ltd., Model: 7000A) and a Gerstel Multi-Purpose MPS autosampler (MPS 2XL; GERSTEL GmbH & Co.). Details of the GC-MS method are provided in *SI Appendix*.

ACKNOWLEDGMENTS. We thank P. S. Fard, V. B. Maisuria, S. Matthews, M. Guo, V. Meola, E. Mahé, and A. Smith for experimental assistance; W. W. Burggren for helpful discussions; K. Wilkinson for access to the ICP-MS; and D. Smith and B. Casley for reviewing the paper. N.T. acknowledges the Canada Research Chair program, the Canada Foundation for Innovation, and the Natural Sciences and Engineering Research Council of Canada. This research was performed using infrastructure of the Integrated Quantitative Biology Initiative, funded by the Quebec government, McGill University, and Canadian Foundation of Innovation project 33122.

1. A. N. Perkins *et al*., Evaluation of potential carcinogenicity of organic chemicals in synthetic turf crumb rubber. *Environ. Res.* **169**, 163–172 (2019).
2. O. Krüger *et al*., New approach to the ecotoxicological risk assessment of artificial outdoor sporting grounds. *Environ. Pollut.* **175**, 69–74 (2013).
3. H. Cheng, Y. Hu, M. Reinhard, Environmental and health impacts of artificial turf: A review. *Environ. Sci. Technol.* **48**, 2114–2129 (2014).
4. M. K. Peterson, J. C. Lemay, S. Pacheco Shubin, R. L. Prueitt, Comprehensive multipathway risk assessment of chemicals associated with recycled ("crumb") rubber in synthetic turf fields. *Environ. Res.* **160**, 256–268 (2018).
5. A. Wik, G. Dave, Occurrence and effects of tire wear particles in the environment–A critical review and an initial risk assessment. *Environ. Pollut.* **157**, 1–11 (2009).
6. C. Marwood *et al*., Acute aquatic toxicity of tire and road wear particles to alga, daphnid, and fish. *Ecotoxicology* **20**, 2079–2089 (2011).
7. S. T. Pochron *et al*., The response of earthworms (*Eisenia fetida*) and soil microbes to the crumb rubber material used in artificial turf fields. *Chemosphere* **173**, 557–562 (2017).
8. Y. Van de Peer, S. Maere, A. Meyer, The evolutionary significance of ancient genome duplications. *Nat. Rev. Genet.* **10**, 725–732 (2009).
9. A. Kapusta, A. Suh, C. Feschotte, Dynamics of genome size evolution in birds and mammals. *Proc. Natl. Acad. Sci. U.S.A.* **114**, E1460–E1469 (2017).
10. D. C. Powell *et al*., Effects of 3,3′,4,4′,5-pentachlorobiphenyl (PCB 126) and 2,3,7,8-tetrachlorodibenzo-p-dioxin (TCDD) injected into the yolks of chicken (*Gallus domesticus*) eggs prior to incubation. *Arch. Environ. Contam. Toxicol.* **31**, 404–409 (1996).
11. S. M. Smith, G. R. Flentke, A. Garic, "Avian models in teratology and developmental toxicology" in *Developmental Toxicology*, J. M. Walker, Ed. (Humana Press, Totowa, NJ, 2012), pp. 85–103.
12. M. Prasek *et al*., Influence of nanoparticles of platinum on chicken embryo development and brain morphology. *Nanoscale Res. Lett.* **8**, 251 (2013).
13. B. Brunstrom, P. O. Darnerud, Toxicity and distribution in chick embryos of 3,3′,4,4′-tetrachlorobiphenyl injected into the eggs. *Toxicology* **27**, 103–110 (1983).
14. V. Hamburger, H. L. Hamilton, A series of normal stages in the development of the chick embryo. *J. Morphol.* **88**, 49–92 (1951).
15. G. L. Semenza, Vasculogenesis, angiogenesis, and arteriogenesis: Mechanisms of blood vessel formation and remodeling. *J. Cell. Biochem.* **102**, 840–847 (2007).
16. US EPA (United States Environmental Protection Agency), "Methods for aquatic toxicity identification evaluations: Phase I toxicity characterization procedures" (EPA 600/6-91/003, US Environmental Protection Agency, Washington, DC, 1991).
17. A. Fournier, C. Feidt, M. A. Dziurla, C. Grandclaudon, C. Jondreville, Transfer kinetics to egg yolk and modeling residue recovered in yolk of readily metabolized molecules: Polycyclic aromatic hydrocarbons orally administered to laying hens. *Chemosphere* **78**, 1004–1010 (2010).
18. T. Shimizu, T. B. Patton, S. A. Husband, Avian visual behavior and the organization of the telencephalon. *Brain Behav. Evol.* **75**, 204–217 (2010).
19. X. Li, W. Berger, C. Musante, M. I. Mattina, Characterization of substances released from crumb rubber material used on artificial turf fields. *Chemosphere* **80**, 279–285 (2010).
20. Y. H. Kim, E. Y. Kim, B. J. Gwag, S. Sohn, J. Y. Koh, Zinc-induced cortical neuronal death with features of apoptosis and necrosis: Mediation by free radicals. *Neuroscience* **89**, 175–182 (1999).
21. W. N. Beyer *et al*., Zinc and lead poisoning in wild birds in the tri-state mining district (Oklahoma, Kansas, and Missouri). *Arch. Environ. Contam. Toxicol.* **48**, 108–117 (2005).
22. J. Bernal, Thyroid hormone receptors in brain development and function. *Nat. Clin. Pract. Endocrinol. Metab.* **3**, 249–259 (2007).
23. C. E. Dean, B. M. Hargis, P. S. Hargis, Effects of zinc toxicity on thyroid function and histology in broiler chicks. *Toxicol. Lett.* **57**, 309–318 (1991).
24. M. Jaishankar, T. Tseten, N. Anbalagan, B. B. Mathew, K. N. Beeregowda, Toxicity, mechanism and health effects of some heavy metals. *Interdiscip. Toxicol.* **7**, 60–72 (2014).
25. S. Preston, N. Coad, J. Townend, K. Killham, G. I. Paton, Biosensing the acute toxicity of metal interactions: Are they additive, synergistic, or antagonistic? *Environ. Toxicol. Chem.* **19**, 775–780 (2000).
26. A. Rai, S. K. Maurya, P. Khare, A. Srivastava, S. Bandyopadhyay, Characterization of developmental neurotoxicity of As, Cd, and Pb mixture: Synergistic action of metal mixture in glial and neuronal functions. *Toxicol. Sci.* **118**, 586–601 (2010).
27. W. J. Birge, O. W. Roberts, J. A. Black, Toxicity of metal mixtures to chick embryos. *Bull. Environ. Contam. Toxicol.* **16**, 314–318 (1976).
28. O. A. Adebambo, P. D. Ray, D. Shea, R. C. Fry, Toxicological responses of environmental mixtures: Environmental metal mixtures display synergistic induction of metal-responsive and oxidative stress genes in placental cells. *Toxicol. Appl. Pharmacol.* **289**, 534–541 (2015).
29. X. Chen, Y. H. Zhu, X. Y. Cheng, Z. W. Zhang, S. W. Xu, The protection of selenium against cadmium-induced cytotoxicity via the heat shock protein pathway in chicken splenic lymphocytes. *Molecules* **17**, 14565–14572 (2012).
30. G. K. Andrews, Regulation of metallothionein gene expression by oxidative stress and metal ions. *Biochem. Pharmacol.* **59**, 95–104 (2000).
31. Y. C. Chien *et al*., Assessment of occupational health hazards in scrap-tire shredding facilities. *Sci. Total Environ.* **309**, 35–46 (2003).
32. G. Ginsberg, B. Toal, T. Kurland, Benzothiazole toxicity assessment in support of synthetic turf field human health risk assessment. *J. Toxicol. Environ. Health A* **74**, 1175–1183 (2011).
33. M. S. Denison, J. P. Whitlock, Jr, Xenobiotic-inducible transcription of cytochrome P450 genes. *J. Biol. Chem.* **270**, 18175–18178 (1995).
34. C. Delescluse, G. Lemaire, G. de Sousa, R. Rahmani, Is CYP1A1 induction always related to AHR signaling pathway? *Toxicology* **153**, 73–82 (2000).
35. D. D. Vakharia *et al*., Effect of metals on polycyclic aromatic hydrocarbon induction of CYP1A1 and CYP1A2 in human hepatocyte cultures. *Toxicol. Appl. Pharmacol.* **170**, 93–103 (2001).
36. E. E. Bessette, M. J. Fasco, B. T. Pentecost, L. S. Kaminsky, Mechanisms of arsenite-mediated decreases in benzo[k]fluoranthene-induced human cytochrome P4501A1 levels in HepG2 cells. *Drug Metab. Dispos.* **33**, 312–320 (2005).
37. J. M. Jacobs *et al*., Effect of arsenite on the induction of CYP1A4 and CYP1A5 in cultured chick embryo hepatocytes. *Toxicol. Appl. Pharmacol.* **168**, 177–182 (2000).
38. T. E. Paton, K. W. Renton, Cytokine-mediated down-regulation of CYP1A1 in Hepa1 cells. *Biochem. Pharmacol.* **55**, 1791–1796 (1998).
39. E. Delaporte, K. W. Renton, Cytochrome P4501A1 and cytochrome P4501A2 are downregulated at both transcriptional and post-transcriptional levels by conditions resulting in interferon-alpha/beta induction. *Life Sci.* **60**, 787–796 (1997).
40. A. A. Caro, A. I. Cederbaum, Role of calcium and calcium-activated proteases in CYP2E1-dependent toxicity in HEPG2 cells. *J. Biol. Chem.* **277**, 104–113 (2002).
41. L. Prigent *et al*., The aryl hydrocarbon receptor is functionally upregulated early in the course of human T-cell activation. *Eur. J. Immunol.* **44**, 1330–1340 (2014).
42. P. Guerre, C. Eeckhoutte, V. Burgat, P. Galtier, The effects of T-2 toxin exposure on liver drug metabolizing enzymes in rabbit. *Food Addit. Contam.* **17**, 1019–1026 (2000).
43. A. Osselaere *et al*., Toxic effects of dietary exposure to T-2 toxin on intestinal and hepatic biotransformation enzymes and drug transporter systems in broiler chickens. *Food Chem. Toxicol.* **55**, 150–155 (2013).
44. R. Tahara, H. C. E. Larsson, Quantitative analysis of microscopic X-ray computed tomography imaging: Japanese quail embryonic soft tissues with iodine staining. *J. Anat.* **223**, 297–310 (2013).